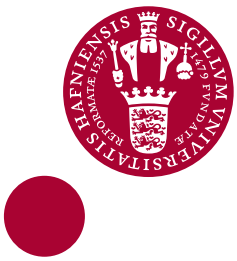

A new NFIA:RAF1 fusion activating the MAPK pathway in pilocytic astrocytoma

Yde, Christina Westmose; Sehested, Astrid; Regué, Àngels Mateu; Østrup, Olga; Scheie, David; Nysom, Karsten; Nielsen, Finn Cilius; Rossing, Maria

Published in:
Cancer genetics and cytogenetics

DOI:
10.1016/j.cancergen.2016.09.002

Publication date:
2016

Document version
Publisher's PDF, also known as Version of record

Cancer Genetics 209 (2016) 440–444

Cancer Genetics

SHORT COMMUNICATION

A new *NFIA:RAF1* fusion activating the MAPK pathway in pilocytic astrocytoma

Christina Westmose Yde [a], Astrid Sehested [b], Àngels Mateu-Regué [a], Olga Østrup [a], David Scheie [c], Karsten Nysom [b], Finn Cilius Nielsen [a], Maria Rossing [a,*]

[a] *Center for Genomic Medicine, Rigshospitalet, Copenhagen University Hospital, Blegdamsvej 9, DK-2100 Copenhagen, Denmark;* [b] *Department of Paediatrics and Adolescent Medicine, Rigshospitalet, Copenhagen University Hospital, Blegdamsvej 9, DK-2100 Copenhagen, Denmark;* [c] *Department of Pathology, Rigshospitalet, Copenhagen University Hospital, Blegdamsvej 9, DK-2100 Copenhagen, Denmark*

Pilocytic astrocytoma (PA) is one of the most common brain cancers among children and activation of the Mitogen-Activated Protein Kinase (MAPK) pathway is considered the hallmark. In the majority of cases, oncogenic *BRAF* fusions or *BRAF* V600E mutations are observed, while *RAF1* or *NF1* alterations are more rarely found. However, in some cases, no apparent cancer driver events can be identified. Here, we describe a novel fusion between the transcription factor nuclear factor 1A (*NFIA*) and Raf-1 proto-oncogene (*RAF1)* in a 5-year old boy with PA. The novel fusion was identified as part of a comprehensive genomic tumor profiling. We show that the *NFIA:RAF1* fusion results in constitutive Raf1 kinase activity, leading to activation of downstream MEK1/2 cascade and increased proliferation of cancer cells. The *NFIA:RAF1* fusion displayed distinct subcellular localization towards the plasma membrane indicative of Raf-1 activation, in contrast to both wild type NFIA and Raf-1, which were localized in the nucleus and cytoplasm, respectively. In conclusion, our data support the existence of rare oncogenic *RAF1* fusions with constitutive Raf-1 activity. This highlights the need for broad genetic testing in order to refine diagnostics of PA and to unravel potential treatment options, e.g. with MEK inhibitors.

Keywords *NFIA:RAF1*, fusion gene, MAPK pathway, pilocytic astrocytoma

Introduction

Pilocytic astrocytoma (PA) is the second most common pediatric cancer diagnosis, constituting about 20% of all pediatric brain tumors and the most common central nervous system tumor (CNS) in the 5–19 year olds (1). PA has a peak incidence in the 0–9 year age group and a favorable 10-year overall survival of around 90% (1–3). The majority of PAs arise in the cerebellum, but a second frequent site is the supratentorial midline, including the optic pathways and the hypothalamic/thalamic regions. PAs are generally slow-growing, classified as World Health Organization (WHO) grade I, and when possible, surgical resection is the treatment of choice, leading to up to 90% progression free survival for cerebellar sites with an achieved complete resection. In case of non- or partially resectable tumors, which constitute the majority of the tumors of the supratentorial midline, many will progress and need non-surgical treatment to control tumor growth and symptoms (4,5). Although PAs are characterized by distinct histologic features, i.e. circumscribed tumors with bipolar cells with long pilocytic processes and Rosenthal fibers, some may show histopathological features resembling gliomas of higher grades, thus making diagnosis of PA challenging (6,7).

Extensive research has recently revealed that the molecular mechanisms leading to PA are associated with the MAPK signaling pathway and constitutive activation is considered the unifying molecular feature of PA (8,9). The most common genetic alterations involve the *BRAF* gene constituting about 80% of all PA cases, where chromosomal rearrangements (e.g.

Received June 3, 2016; received in revised form August 24, 2016; accepted September 8, 2016.

* Corresponding author.
E-mail address: caroline.maria.rossing@regionh.dk

2210-7762/$ - see front matter
http://dx.doi.org/10.1016/j.cancergen.2016.09.002

KIAA1549:BRAF or *FAM131B:BRAF*) or *BRAF* mutations are found (10). In addition, mutations in *KRAS* and in *NF1* have been identified in PA. Previously, no genetic alterations in the MAPK pathway were identified in around one fifth of the PA patients. However, recent high throughput molecular analysis for somatic screening of PAs has revealed novel alterations in *FGFR1* and *NTRK2*, supporting that the genetic alterations in PA are solely linked to the MAPK pathway (9,11). More recently, a fusion between *SRGAP3:RAF1* was identified in a PA patient, showing that translocations involved in PA are not limited to the *BRAF* gene (11).

Materials and methods

Case report

A boy was diagnosed just before his two-year birthday with diencephalic syndrome, severe behavioral disturbance and a large supratentorial midline tumor involving the hypothalamus, basal ganglia and medial temporal lobes bilaterally, measuring 7×3.8 cm. An open biopsy was performed, leading to the diagnosis of PA WHO grade 1. To manage the diencephalic syndrome, a percutaneous endoscopic gastrostomy tube was inserted and he was initially treated with vincristine-carboplatin-etoposide. Due to tumor progression, treatment was changed after six months to vincristine-cyclophosphamide-cisplatin, leading to six months of stable disease. However, after 12 months of therapy the tumor progressed, necessitating placement of a bi-frontal ventriculo-peritoneal shunt. Therapy was changed to vinblastine in combination with bevacizumab, which led to both clinical and radiological improvements but progression occurred within 18 months upon initiation of vinblastin-avastin therapy.

Identification and verification of the *NFIA:RAF1* fusion

RNA was purified from tumor tissue preserved in RNALater (Life Technologies) using total AllPrep DNA/RNA purification kit (Qiagen) and RNA-sequencing was done using TruSeq Stranded Total RNA Library Prep Kit and sequenced on a HiSeq2500 (Illumina). FusionMap bioinformatics tool was used for screening of fusion transcripts (12). Verification by RT-PCR was performed (Primer sequences are available on request). An in-house non-CNS tumor was used as negative control. RT-PCR product was sequenced by Sanger sequencing using an ABI 3730 DNA Analyzer (Applied Biosystems).

Molecular characterization of the *NFIA:RAF1* fusion

HEK293 cells were cultured in DMEM supplied with 10% FBS and penicillin/streptomycin (Invitrogen) and seeded in 6-well plates. Cells were transfected with empty vector, EV (pCMV6-Entry-FLAG, Origene), wild type *NFIA* (pCMV6-NFIA-FLAG, Origene), wild type *RAF1* (pCMV6-RAF1-FLAG, Origene), *NFIA:RAF1* (cDNA cloned into pCMV6-Entry-FLAG) (Primer sequences are available on request). Transfection was done using FuGene Transfection Reagent (Promega) according to manufacturer's recommendations. At 24 hours following transfection, western blot analysis was performed as previously described (13) with antibodies against Raf-1 (#12552; Cell Signaling Technologies) and GAPDH (sc-22778, Santa Cruz Biotecnologies). Transfected HEK293 cells were stimulated for 10 minutes with 10 ng/ml human recombinant epidermal growth factor (EGF) (R&D Systems), and western blot analysis was performed using antibodies against phospho-Ser221-MEK1/2 (#2338; Cell Signaling Technologies), MEK1/2 (#8728; Cell Signaling Technologies). HeLa cells were cultured in DMEM supplied with 1 mM sodium pyruvate, 10% FBS and penicillin/streptomycin (Invitrogen) and seeded in 96-well plates in growth medium without FBS for serum starvation. Cells were transfected using FuGene Transfection Reagent (Promega) and 3 days after transfection, cell growth was measured with MTT assay (Roche). Cell growth was calculated relative to EV transfected cells.

Subcellular protein fractionation analysis

HeLa cells were plated at 30% confluency in 6-well dishes and were transfected 6 hours after with pcDNA6-FLAG-RAF1 or pcDNA6-FLAG-NFIA-RAF1 constructs using FuGene (Promega) following the manufacturers protocol. After 48 hours cells were collected and cytoplasmic and membrane subcellular protein fractionation was performed using Cytoplasmic Extraction Buffer (CEB) and Membrane Extraction Buffer (MEB) from Subcellular Protein Fractionation Kit for Cultured Cells (Thermo Fisher Scientific). Samples were analyzed by Western Blot using anti-FLAG M2 antibody (Sigma).

Microscopy for subcellular localization

HeLa cells were plated at 40% confluency in 35 mm No. 1.5 coverglass Glass Bottom Microwell Dishes (MatTek Corporation) and transfected after 6 hours with pCMV6-Entry-NFIA-FLAG, pCMV6-Entry-RAF1-FLAG or pCMV6-Entry-NFIA:RAF1-FLAG constructs using FuGene Transfection Reagent (Promega). After 24 hours, cells were fixed in 4% paraformaldehyde for 15 minutes, permeabilized in 0.1% Triton X-100 for 10 minutes, incubated with Image-iT FX Signal Enhancer (Thermo Fisher Scientific) for 30 minutes and blocked in 3% BSA 0.1% Triton X-100 for 1 hour at room temperature. Dishes were then incubated with 1:10,000 mouse monoclonal anti-FLAG M2 antibody (Sigma) overnight at 4 °C. The day after, samples were incubated with 1:1000 secondary donkey anti-mouse Alexa Fluor 488 (Thermo Fisher Scientific) and Alexa Fluor 568 Phalloidin (Thermo Fisher Scientific) for 1 hour at room temperature. Fluoroshield with DAPI mounting media (Sigma) was added to the dishes and images were acquired with Zeiss ELYRA PS.1 LSM780 microscope. The experiment was repeated using HEK293 cells (data not shown due to suboptimal adherence of cells to cover glass dishes).

Results and discussion

In search for a targeted treatment, the patient was stereotactically re-biopsied and comprehensive genomic profiling was carried out to unravel the genetic alterations driving the neoplastic growth in this patient. The comprehensive genomic

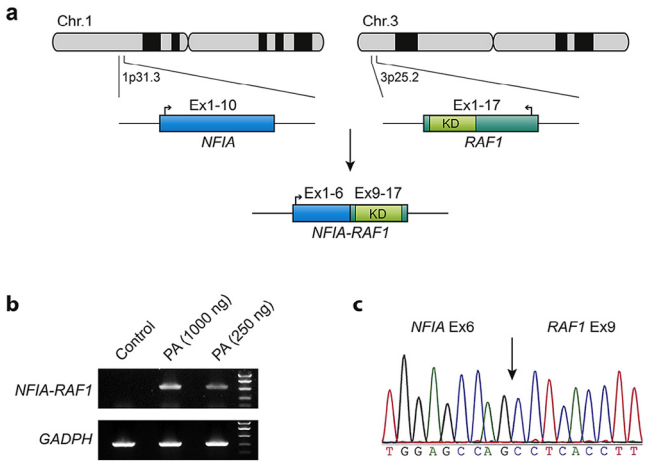

Figure 1 Identification of a novel *NFIA:RAF1* fusion in pilocytic astrocytoma. (a) Graphic illustration of translocation between the chromosomal regions 1q31.3 and 3p25.2, resulting in fusion between *NFIA* (NM_001134673.3) exons 1–6 and *RAF1* (NM_002880.3) exons 9–17, including the Raf-1 kinase domain. (b) RT-PCR with primers in *NFIA* exon 6 and *RAF1* exon 9 resulted in a 406 bp PCR product. An in-house non-CNS tumor was used as negative control. (c) The junction was verified by Sanger sequencing of the RT-PCR product.

profiling included whole exome sequencing of purified tumor DNA (SureSelect Illumina), SNP array (Affymetrix), methylation array (450K Illumina) and purified tumor RNA was subjected to RNA sequencing (RNA-Seq Illumina strand specific) and expression array (Affymetrix U133 plus 2.0). Initial screening for common genetic alterations in PA (*BRAF*, *KRAS*, *NF1*) was negative. However, a broad search for fusion transcripts based on RNA-Seq data revealed a novel fusion between the transcription factor nuclear factor 1A (*NFIA*) and Raf-1 proto-oncogene (*RAF1*). A translocation between the chromosomal regions 1q31.3 and 3p25.2 was identified, resulting in fusion between *NFIA* exons 1–6 and *RAF1* exons 9–17, including the complete coding sequence of the Raf1 kinase domain (Figure 1a). The breakpoint region was validated by Sanger sequencing (Figure 1b and c). In comparison, the breakpoint between the previously identified fusion *SRGAP3:RAF1* is located by joining exons 1–12 of *SRGAP3* to exons 10–17 of *RAF1* (11). The srGAP3:Raf-1 fusion protein was demonstrated to be hyperactive, presumably by a molecular mechanism involving lack of the N-terminal autoinhibitory region of Raf-1 (11,14), pointing to a similar mechanism of action for the NFIA:Raf-1 fusion protein.

To explore the expression level of *RAF1* mRNA in the PA specimen in comparison with other PA expression profiles, we examined two large online available datasets containing HG-U133_Plus_2 expression array data from 47 (E-GEOD-73066) and 49 (E-GEOD-44971) PA patients, respectively (15,16). *RAF1* was not differentially expressed (data not shown), indicating that activation of Raf-1, rather than its overexpression, is the cancer driver event in the patient. Hence, we sought to clarify if the *NFIA:RAF1* fusion results in constitutive activity of Raf-1. HEK293 cells were transfected with wild type *NFIA*, wild type *RAF1*, or the *NFIA:RAF1* fusion gene (Figure 2a). To explore if the fusion protein causes increased Raf-1 kinase activity, we examined the phosphorylation of MEK1, a Raf-1 substrate. Elevated phosphorylation of endogenous MEK1/2 was observed in the *NFIA:RAF1* transfected cells, compared to cells with either of the fusion partners (Figure 2b). The phosphorylation caused by the fusion was shown to be equally potent as treatment of HEK293 cells with epidermal growth factor (EGF), a well-described activator of the MAKP pathway (17) (Figure 2b), demonstrating that the *NFIA:RAF1* fusion results in a constitutive activation of the MAPK pathway. To investigate if the AKT/mTOR pathway was equally activated by the fusion protein, western blot analysis of phospho-S6 was performed after transfection; however, these results did not reveal any significant changes in S6 phosphorylation levels (data not shown), supporting the notion that the NFIA:Raf-1 fusion protein primarily activates the MAPK pathway. To determine the effect of the fusion on cell growth, we performed an *in vitro* proliferation assay, showing a significant increase in cell growth of cancer cells transfected with the fusion (Figure 2c). MAPK pathway activation by EGF stimulation of serum starved HeLa cells resulted in 2.3-fold growth stimulation (data not shown).

To further characterize the novel fusion protein, we explored the subcellular localization of the NFIA:Raf-1 protein. By performing fractionation of the cytoplasmic and membrane components in transfected HeLa cells, it was evident that while wild type Raf1 kinase was enriched in the cytoplasmic fraction, the NFIA:Raf-1 fusion was clearly enriched in the membrane fraction (Figure 2d). Immunofluorescence microscopy was used to further investigate the subcellular localization of the different constructs. The transcription factor NFIA was localized in the nucleus (Figure 2e), while wild type Raf-1 was located in the cytoplasm (Figure 2f). Interestingly, it was confirmed that NFIA:Raf-1 fusion protein displayed distinct subcellular localization with accumulation towards the plasma membrane (Figure 2g), supporting the notion of constitutive Raf-1 activation in the fusion as it has previously been demonstrated that activated Raf-1 is recruited to the membrane (18,19).

It is well established that PAs harbor the *KIAA1549:BRAF* fusion and the majority of the cerebellar (80%) versus noncerebellar (50–55%) PAs are driven by this fusion (20). In line with this distribution, our novel *NFIA:RAF1* fusion was identified in a noncerebellar PA. Our findings of a novel RAF1 fusion and its relation to constitutive MEK activation support the role of MAPK pathway as a key player in the tumorigenesis of PA, as well as contribute to the current knowledge and molecular complexity of oncogenes in PA. To ensure an optimized and tailored treatment, it is crucial to substantiate the different genetic alterations within the MAPK pathway. To unravel the remaining 20–50% that do not harbor the frequent *KIAA1549:BRAF* fusion, wide molecular screening, i.e. DNA and RNA-sequencing, and SNP-array should be carried out on therapy resistant cases. The identification of the novel *NFIA:RAF1* fusion gene emphasizes the feasibility of comprehensive genomic profiling for identification of rational treatment targets (21). Therapy with MEK inhibitors, which are currently in clinical phase 1 and phase 2 trials (22), provides hope for precision medicine for the patients suffering from a more rare PA with e.g. *RAF1* alterations. Our patient, who is now 6 years old, was not eligible for open European MEK inhibitor trials, but was granted treatment with the MEK inhibitor trametinib on a compassionate use. Results from the MRI scan

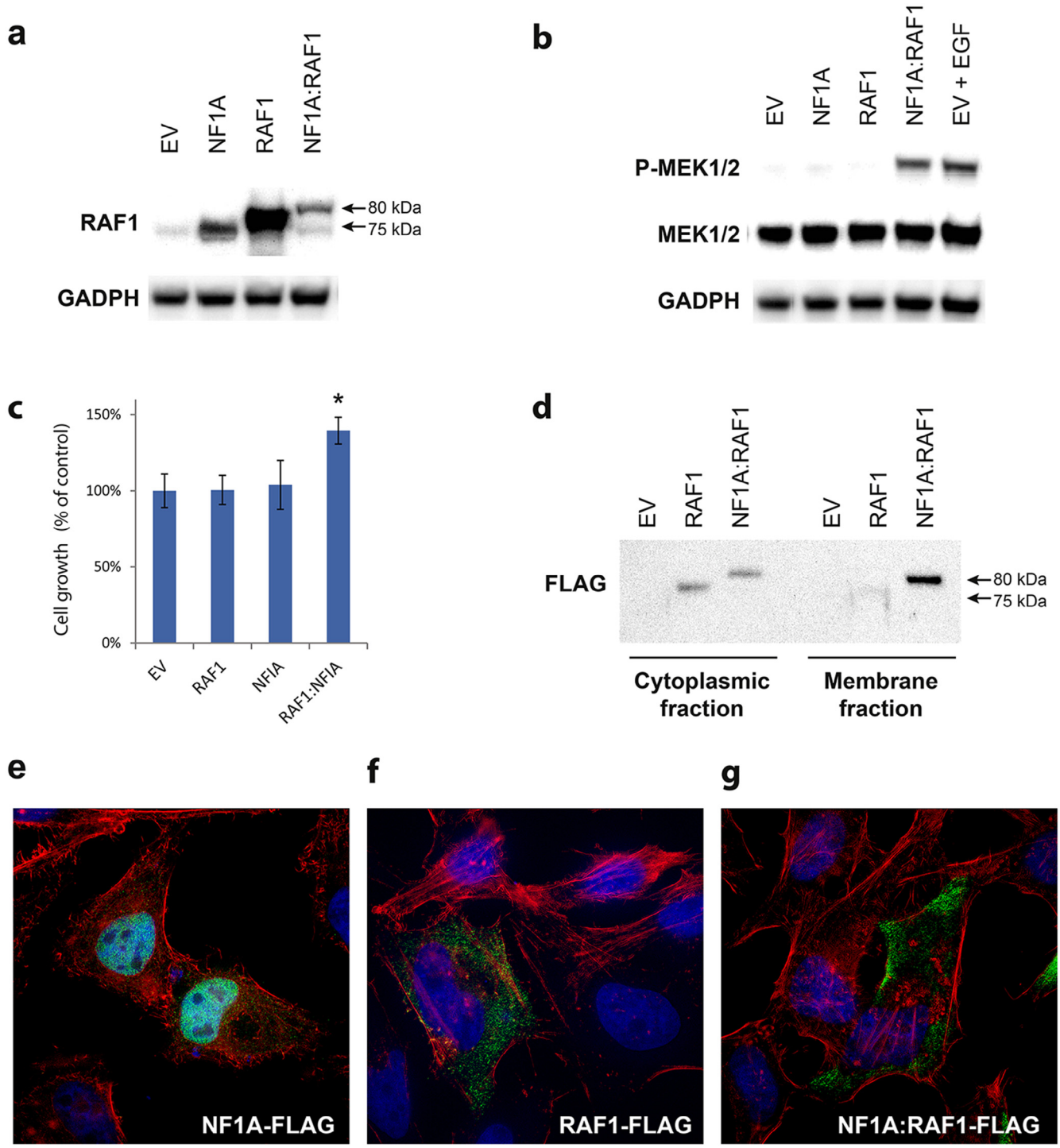

Figure 2 Functional characterization and subcellular localization of *NFIA:RAF1* fusion. (a) HEK293 cells were transfected with empty vector, EV (pCMV6-Entry-FLAG), wild type *NFIA* (pCMV6-NFIA-FLAG), wild type *RAF1* (pCMV6-RAF1-FLAG), *NFIA:RAF1* (cDNA cloned into pCMV6-Entry-FLAG). Western blot analysis was performed using antibodies against Raf-1 and GAPDH. The molecular weight of the fusion protein was calculated to 80 kDa, while the endogenous Raf-1 is 75 kDa as depicted. (b) HEK293 cells were transfected as described above, or stimulated for 10 minutes with 10 ng/ml human recombinant epidermal growth factor (EGF) as positive control for activated MAPK pathway. Antibodies against phospho-Ser221-MEK1/2, MEK1/2 were used. (c) Cell growth of transfected HeLa cells was measured 3 days after transfection. Cell growth is calculated relative to EV transfected cells. Error bars shown are standard error of the mean (SEM) and the asterisk denotes statistical significance ($P = 0.049$) compared to EV. (d) HeLa cells were transfected with EV, wild type RAF1 or *NFIA:RAF1* constructs and fractionation into cytoplasmic and membrane fractions was performed as described in the Materials and Methods section. Western blotting was performed using an antibody against FLAG-tag. (e–g) Transfected HeLa cells were fixed and stained for FLAG-tag (green) indicating the FLAG-tagged constructs; NFIA-FLAG, RAF1-FLAG and NFIA:RAF1-FLAG, F-actin (red), reflecting the localization of the cellular membrane and nucleus (blue). (For interpretation of the references to color in this figure legend, the reader is referred to the web version of this article.)

three and six months after initiating trametinib showed stable disease and the treatment is currently ongoing.

Conflict of interest

The authors declare no conflict of interest.

Acknowledgments

We thank Christina Ringø, Stine Østergaard and Miriam Yan Juk Guo for excellent laboratory assistance.

References

1. Ostrom QT, Gittleman H, Fulop J, et al. CBTRUS statistical report: primary brain and central nervous system tumors diagnosed in the United States in 2008-2012. Neuro Oncol 2015;17(suppl 4):iv1–iv62.
2. Louis DN, Ohgaki H, Wiestler OD, et al. The 2007 WHO classification of tumours of the central nervous system. Acta Neuropathol 2007;114:97–109.
3. Ohgaki H, Kleihues P. Epidemiology and etiology of gliomas. Acta Neuropathol 2005;109:93–108.
4. Dirven CM, Mooij JJ, Molenaar WM. Cerebellar pilocytic astrocytoma: a treatment protocol based upon analysis of 73 cases and a review of the literature. Childs Nerv Syst 1997;13:17–23.
5. Ichimura K, Nishikawa R, Matsutani M. Molecular markers in pediatric neuro-oncology. Neuro Oncol 2012;14(suppl 4):iv90–iv99.
6. Coons SW, Johnson PC, Scheithauer BW, et al. Improving diagnostic accuracy and interobserver concordance in the classification and grading of primary gliomas. Cancer 1997;79:1381–1393.
7. van den Bent MJ. Interobserver variation of the histopathological diagnosis in clinical trials on glioma: a clinician's perspective. Acta Neuropathol 2010;120:297–304.
8. Jones DT, Gronych J, Lichter P, et al. MAPK pathway activation in pilocytic astrocytoma. Cell Mol Life Sci 2012;69:1799–1811.
9. Jones DT, Hutter B, Jager N, et al. Recurrent somatic alterations of FGFR1 and NTRK2 in pilocytic astrocytoma. Nat Genet 2013;45:927–932.
10. Jones DT, Kocialkowski S, Liu L, et al. Tandem duplication producing a novel oncogenic BRAF fusion gene defines the majority of pilocytic astrocytomas. Cancer Res 2008;68:8673–8677.
11. Jones DT, Kocialkowski S, Liu L, et al. Oncogenic RAF1 rearrangement and a novel BRAF mutation as alternatives to KIAA1549:BRAF fusion in activating the MAPK pathway in pilocytic astrocytoma. Oncogene 2009;28:2119–2123.
12. Ge H, Liu K, Juan T, et al. FusionMap: detecting fusion genes from next-generation sequencing data at base-pair resolution. Bioinformatics 2011;27:1922–1928.
13. Jonson L, Christiansen J, Hansen TV, et al. IMP3 RNP safe houses prevent miRNA-directed HMGA2 mRNA decay in cancer and development. Cell Rep 2014;7:539–551.
14. Cin H, Meyer C, Herr R, et al. Oncogenic FAM131B-BRAF fusion resulting from 7q34 deletion comprises an alternative mechanism of MAPK pathway activation in pilocytic astrocytoma. Acta Neuropathol 2011;121:763–774.
15. Lambert SR, Witt H, Hovestadt V, et al. Differential expression and methylation of brain developmental genes define location-specific subsets of pilocytic astrocytoma. Acta Neuropathol 2013;126:291–301.
16. Zakrzewski K, Jarzab M, Pfeifer A, et al. Transcriptional profiles of pilocytic astrocytoma are related to their three different locations, but not to radiological tumor features. BMC Cancer 2015;15:778.
17. Bunone G, Briand PA, Miksicek RJ, et al. Activation of the unliganded estrogen receptor by EGF involves the MAP kinase pathway and direct phosphorylation. EMBO J 1996;15:2174–2183.
18. Jelinek T, Dent P, Sturgill TW, et al. Ras-induced activation of Raf-1 is dependent on tyrosine phosphorylation. Mol Cell Biol 1996;16:1027–1034.
19. Rizzo MA, Shome K, Watkins SC, et al. The recruitment of Raf-1 to membranes is mediated by direct interaction with phosphatidic acid and is independent of association with Ras. J Biol Chem 2000;275:23911–23918.
20. Horbinski C. To BRAF or not to BRAF: is that even a question anymore? J Neuropathol Exp Neurol 2013;72:2–7.
21. Aronson SJ, Rehm HL. Building the foundation for genomics in precision medicine. Nature 2015;526:336–342.
22. Rusconi P, Caiola E, Broggini M. RAS/RAF/MEK inhibitors in oncology. Curr Med Chem 2012;19:1164–1176.